



Optical response of grain boundaries in upgraded metallurgical-grade silicon for photovoltaics

Fude Liu^{a,*}, C.-S. Jiang^b, H. Guthrey^{b,c}, S. Johnston^b, M.J. Romero^b, B.P. Gorman^c, M.M. Al-Jassim^b

^a Department of Mechanical Engineering, The University of Hong Kong, Pokfulam Road, Hong Kong, China

^b National Center for Photovoltaics, National Renewable Energy Laboratory, Golden, CO 80401, United States

^c Department of Metallurgical and Materials Engineering, Colorado School of Mines, CO 80401, United States

ARTICLE INFO

Article history:

Received 21 December 2010

Received in revised form

6 April 2011

Accepted 21 April 2011

Available online 18 May 2011

Keywords:

Upgraded metallurgical-grade silicon (UMG-Si)

Photovoltaics

Grain boundaries

Light emission

Impurities

Characterization

ABSTRACT

Using upgraded metallurgical-grade silicon (UMG-Si) is a cost-effective and energy-efficient approach for the production of solar cells. Grain boundaries (GBs) play a major role in determining the device performance of multicrystalline Si (mc-Si) solar cells. In this study two UMG-Si wafers, one from the middle part of a brick and the other from the top part of the same brick, were investigated. An excellent correlation was found between the grain misorientation and the corresponding optical response of GBs as indicated by photoluminescence (PL) imaging, electron backscattered diffraction (EBSD), and cross-sectional transmission electron microscopy (TEM). In addition, the PL features at random GBs depend also on the impurity levels in the wafer. In particular the PL emission was greatly enhanced in the narrow regions close to the random GB in the top wafer, which is an interesting phenomenon that may have potential application in high efficiency light-emission diodes (LEDs) based on Si.

© 2011 Elsevier B.V. All rights reserved.

1. Introduction

So far, solar modules made of Si wafers (multicrystalline ones in particular) have dominated the solar market. Si wafers (monocrystalline and multicrystalline) are traditionally made of electronic-grade silicon (EG-Si), which is obtained from metallurgical-grade silicon (MG-Si) via complex purification processes [1]. Using upgraded metallurgical-grade silicon (UMG-Si) is regarded as a cost-effective and energy-efficient approach for the production of Si wafers. Since Si wafers are one of the major costs of solar modules, UMG-Si will be one of the technologies that help drive down the cost of solar energy. Although UMG-Si is three orders of magnitude less pure compared with EG-Si, it has been demonstrated that the performance of high-quality UMG-Si solar cells can be comparable to that of typical EG-Si counterparts [2]. However, the UMG-Si wafer quality needs to be further improved in order to have a high market penetration. Grain boundaries (GBs) play an important role in determining the device performance of solar cells made of multicrystalline silicon (mc-Si), because GBs enhance minority carrier recombination and reduce majority carrier transport. In addition GBs are possible shunting paths and also the preferred sites for extrinsic impurities, which is

particularly so for UMG-Si because of its impurity levels. Note also that wafers sliced from the top part of ingots fabricated by the directional solidification process contain higher impurity levels, because impurity elements (except B) have distribution coefficients much less than one [1]. Therefore, it is necessary to have a systematic study of GBs and their behaviors in UMG-Si.

Photoluminescence (PL) is an important technique for measuring the defect density and lifetime in association with the material purity and crystalline quality of semiconductors [3]. Compared with other PL techniques such as PL spectroscopy and PL mapping, PL imaging has recently been demonstrated to be a rapid contactless characterizing technique with relatively high spatial resolution, which makes it a useful tool for studying mc-Si wafers [4,5]. On the other hand, electron backscattered diffraction (EBSD) is a technique that is often used to examine the crystallographic orientation of crystalline materials from electron-diffraction patterns [6]. Combining these two techniques will then allow us to determine the correlation between the PL behaviors and the misorientation of GBs in UMG-Si wafers. In addition, transmission electron microscopy (TEM) specimens can be prepared from specifically selected GBs using a dual-beam focused ion beam (FIB) workstation; the specimen can then be further investigated by TEM at high resolution.

We have recently investigated the structural and electronic/electrical properties of individual GBs in polycrystalline thin films with grain sizes in micrometer order, where the depletion of

* Corresponding author. Tel.: +852 2859 2631; fax: +852 2858 5415.
E-mail address: fordliu@hku.hk (F. Liu).

carriers on the GBs was measured by scanning capacitance microscopy (SCM) due to its fine resolution of tens of nanometers [7,8]. The electrical and structural properties were well correlated. Due to the large grain sizes of mc-Si we in this paper employed PL imaging for the electrical property study, and found consistent relationship between the structural and electrical properties in these Si-based materials.

2. Experimental

Two UMG-Si wafers (B doped with a size of $156 \times 156 \text{ mm}^2$), one sliced from the middle part of a brick and the other from the top part of the same brick, were examined. The wafers were first etched in HF ($\sim 1\%$) to remove the native oxide, and were then submerged in a methanol-iodine solution [9]. The surface passivation can reduce surface recombination and allow for dramatically improved PL imaging of the bulk wafer. The wafers were imaged by PL imaging while they were still in the solution. All measurements were carried out at room temperature.

Based on the PL results, we selected a few typical GBs according to their different optical response. The same GBs (marked by a paper mask) were then studied by plan-view EBSD mapping to get grain misorientation between two adjacent grains. The EBSD mapping was done with an SEM microscope (Hitachi

S-4300N) at 20 kV, a sample tilt angle of 70° , and a working distance of 15 mm. In addition, specifically selected cross-sectional TEM specimens were prepared using a focused-ion-beam (FIB) workstation (FEI-Nova 200 Dual Beam) at normal operating parameters. These specimens were then further investigated using a TEM microscope (FEI-T30) at 200 kV by bright- and dark-field imaging, selected-area diffraction (SAD), and energy-dispersive X-ray spectroscopy (EDX). The same procedure was applied to both the middle wafer and the top wafer.

The PL imaging setup and its working principles are illustrated in Fig. 1. The wafer is illuminated by 810 nm light from the back side to avoid interference between the incident light and emitted light. Electrons are excited from the valence band to the conduction band. The electrons then relax to the conduction band edge, and some emit light at $\sim 1100 \text{ nm}$ as they recombine back to the valence band. This emission passes through the filter and is detected by the Si charge-coupled device (CCD) camera. The illumination intensity is equivalent to 1 Sun, and the data acquisition time is 600 s.

3. Results and discussion

The optical image, PL image, and EBSD maps of the middle wafer are shown in Fig. 2. A paper mask (hole diameter = 8 mm) is used to mark the region of interest. From the optical image (Fig. 2(a)), we can see clearly the GBs. Five different GBs (1–5) and three different regions (I–III) are studied in detail as shown in Fig. 2(b) and Fig. 2(c), respectively. Although the PL image was taken from the same region as that of the optical counterpart, we can see that different GBs show different optical responses. The inset in Fig. 2(b) displays the image intensity profile from the region indicated by the rectangular frame in the PL image, where GBs with different PL intensities are marked by arrows and numbers. The EBSD maps obtained from three regions (I–III) are displayed in Fig. 2(c). The EBSD map is color-coded with the inverse pole figure (IPF) coloring in the sample normal direction Z_0 . Also shown is the grain misorientation (angle and axis of rotation) between adjacent grains. $\Sigma 3$ GBs are indicated by white lines; the misorientation to all the $\Sigma 9$ GBs in this study was experimentally measured to be $\sim 39.5^\circ$ and $\langle 011 \rangle$. Comparing the PL image and

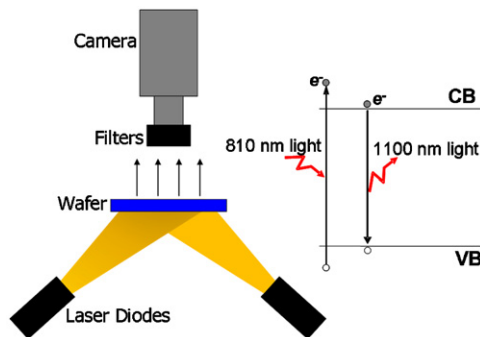


Fig. 1. Schematic of the PL imaging setup and its working principles.

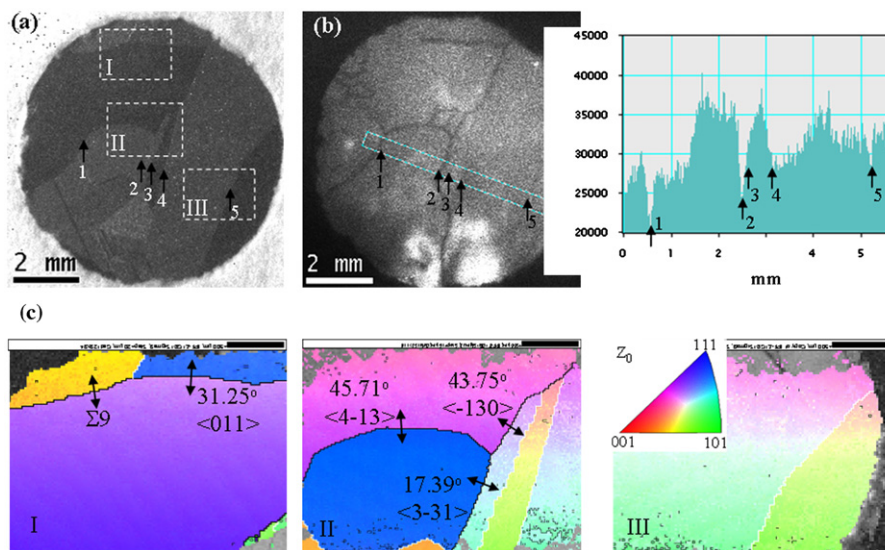


Fig. 2. Middle wafer. (a) Optical image. A paper mask (hole diameter = 8 mm) is used to mark the region of interest. Five different GBs (1–5) and three different regions (I–III) are studied in detail in (b) and (c), respectively. (b) PL image of the same region as in (a). The inset displays the image intensity profile from the region indicated by the rectangular frame in the PL image. GBs with different PL intensities are indicated by arrows and numbers. (c) EBSD maps obtained from three different regions (I–III) as shown in (a). The inset in panel III is the color-coding legend. Also shown is the grain misorientation between adjacent grains ($\Sigma 3$ GBs are indicated by white lines). (For interpretation of the references to color in this figure legend, the reader is referred to the web version of this article.)

Download English Version:

<https://daneshyari.com/en/article/78812>

Download Persian Version:

<https://daneshyari.com/article/78812>

[Daneshyari.com](https://daneshyari.com)